Applied Thermal Engineering 31 (2011) 3226–3234

Contents lists available at ScienceDirect

Applied Thermal Engineering

journal homepage: www.elsevier.com/locate/apthermeng

Characteristics of flow distribution in compact parallel flow heat exchangers, part I: Typical inlet header

Chi-Chuan Wang [a], Kai-Shing Yang [b], Jhong-Syuan Tsai [c], Ing Youn Chen [c,*]

[a] Department of Mechanical Engineering, National Chiao Tung University, Hsinchu 300, Taiwan, ROC
[b] Green Energy & Environment Research Labs, Industrial Technology Research Institute, Hsinchu 310, Taiwan, ROC
[c] Department of Mechanical Engineering, National Yunlin University of Science and Technology, Yunlin 640, Taiwan, ROC

ARTICLE INFO

Article history:
Received 23 February 2011
Accepted 2 June 2011
Available online 12 June 2011

Keywords:
Flow distribution
Header
Parallel flow heat exchangers

ABSTRACT

This study experimentally and numerically investigates the single-phase flow into parallel flow heat exchangers with inlet and outlet rectangular headers having square cross section and 9 circular tubes. The effects of inlet flow condition, tube diameter, header size, area ratio, flow directions (Z and U-type), as well as the gravity are investigated. The experimental results indicate that flow distribution for U-type flow is more uniform than Z-type flow. Depending on the inlet volumetric flow rate, the flow ratio at the first several tubes can be lower than 50% of the last tube for Z-type arrangement, and this phenomenon becomes more and more pronounced with the rising velocity at the intake conduit. The mal-distribution can be eased via reducing the branching tube size or increasing the entrance settling distance at the intake conduit. It is found that the influence of gravity on mal-distribution is negligible and the mal-distribution is associated with the jet flow pattern.

© 2011 Elsevier Ltd. All rights reserved.

1. Introduction

Flow distribution from a header into parallel channels applicable to heat exchangers is frequently encountered in heat transfer equipments, such as condensers, evaporators, boilers, solar energy flat-plate collectors, and cooling system of nuclear reactor. Apparently, the flow rates of single-phase distribution through the parallel channels are often not uniform which could greatly affect the heat transfer performance, these heat transfer devices may suffer from significant performance drop subject to mal-distribution. Therefore, the issue of uniform flow distribution has recently received growing attentions for the heat exchanger design. The uneven distribution in parallel channels could be related to the stream velocity in the header (or manifold), size of the header, diameter of the tube, location and size of inlet port to the header, flow direction, orientation of the channels and the like. Thus, it is very imperative to understand the flow distribution phenomena in the header and parallel channels as far as performance is concerned.

The single-phase distribution in a parallel flow heat exchanger had been studied by several investigators. The single-phase distribution mechanism and calculation procedure are normally better understood than two-phase flow [1]. However, until now, there still lacks of general methodology for improving the flow distribution at header-tube junctions due to the complex interactions amid geometrical configurations and inlet flow conditions at the inlet header.

1.1. Parameters for counting the flow distribution

For counting the flow distribution among the parallel tubes, the dimensionless parameters, β_i, $\overline{\beta}$ and Φ are used for evaluating the flow distribution. Their definitions are given as following:

$$\beta_i = Q_i/Q \tag{1}$$

Where β_i denotes the flow ratio for ith tube, Q_i represents volume flow rate for ith tube (m^3/s), and Q is total volume flow rate (m^3/s).

To characterize the influence, Chiou [2] had used the concept of standard deviation to define the non-uniformity, Φ as:

$$\Phi = \sqrt{\frac{\sum_{i=1}^{N}(\beta_i - \overline{\beta})^2}{N}} \tag{2}$$

Where N is the number of total tubes in the parallel flow heat exchanger and $\overline{\beta}$ is the average flow ratio for the total tubes which is defined as $\overline{\beta} = (\sum_{i=1}^{N}\beta_i)/N$. The larger value of Φ indicates the higher non-uniformity.

* Corresponding author. Tel.: +886 5 5342601; fax: +886 5 5312062.
E-mail address: cheniy@yuntech.edu.tw (I.Y. Chen).

1359-4311/$ – see front matter © 2011 Elsevier Ltd. All rights reserved.
doi:10.1016/j.applthermaleng.2011.06.004

Nomenclature

A	cross-sectional flow area (m^2)
AR	header-tube flow area ratio ($(N\pi D^2/4)/A$)
D	inner tube diameter (m)
f	fanning friction factor
g	gravity (m/s^2)
G	mass flux (kg/m^2 s)
h	vertical height (m)
N	number of total tubes
Q_i	volume flow rate for ith tube (m^3/s)
Q	total volume flow rate (m^3/s)

Greek symbols

β_i	flow ratio for ith tube defined in Eq. (1)
$\overline{\beta}$	average flow ratio for the total tubes
ΔL	length for ΔP measurement
ΔP	measured pressure drop (N/m^2)
ρ	density (kg/m^3)
Φ	non-uniformity defined in Eq. (2)

Subscript

f	friction
i	ith

1.2. Factors for affecting the flow distribution

From the previously reported results of the cited references, the trends for the flow distribution affected by several operating factors are briefly discussed in the following.

1.2.1. Flow area ratio

For evaluating the effect of the header size, the header-tube flow area ratio (AR) had been defined as the ratio of the header cross-sectional area (A) to the total cross-sectional area of all branch tubes ($AR = (N\pi D^2/4)/A$). Datta and Majumdar [3] had utilized the numerical method to calculate the flow distribution for two different outlet locations from the downstream header. Their results showed that the flow non-uniformity is increased as area ratio is increased.

Bajura and Jones [4] had theoretically analyzed the flow distribution and proposed a model for the prediction of flow distribution. The predicted values were compared with the measured data. For obtaining a more uniform flow distribution, $AR < 1$ is suggested for design.

Choi and Cho [5] had numerically investigated the flow distribution for electronic cooling with different AR values (4, 8, and 16) for a Reynolds number of 50, the case of $AR = 4$ produced the best coolant distribution. When the flow enters the tubes from the header, the eddy flow appeared at the inlet section for each tube, yet the engendered eddy flow becomes more pronounced with the rise of area ratio, leading to conspicuous mal-distribution.

Tong et al. [6] numerically examined the influences of cross section area of the header. The simplest way for attaining the outflow uniformity is to enlarge the headers for increasing their cross section area or reducing the flow area ratio.

1.2.2. Flow direction

The inlet and the exit flows may be located at the same side or the opposite side of the heat exchanger as called Z-type (parallel flow), or U-type (reverse flow) as shown in Fig. 1. U-type and Z-type flow directions are the most commonly used configurations for parallel flow heat exchanger and normally the flow distribution of U-type is more uniform than Z-type at the same flow area ratio [3]. This is because the pressure differences between the inlet header and outlet header for all the tubes are more evenly distributed for U-type than that of Z-type [7].

1.2.3. Inlet velocity to the header or entrance effect

In general, the higher inlet velocity to the header leads to a higher pressure drop at the header entrance. This is primarily associated with appreciable pressure drop with the jet flow into the header, thereby reducing the flow rate into branching tubes near the header entrance. The inlet velocity is affected by the total flow rate and the cross section area at the entrance. Choi and Cho [5] indicated that the flow rate for the downstream branching tubes is significantly increased with the rise of inlet total flow rate to the header, and consequently the flow rate to the tubes near the entrance is decreased.

Recently, Tong et al. [6] utilized the numerical simulation and indicated the larger size for the inlet tube having a better distribution, while the smaller inlet size could induce jet flow at the entrance and cause reverse flow in the branching tubes at the upstream. The jet flow phenomenon becomes more significant with a higher inlet flow rate or a smaller tube size at the entrance to the header.

1.2.4. Flow resistance

In a dividing header, the main fluid stream is decelerated due to the loss of both fluid and momentum through parallel tubes, thus causing a rise in pressure in the direction of flow. However, the frictional effect would cause a decrease of pressure in the flow direction of header and tubes.

Bajura and Jones [4] inserted a small orifice inside the parallel tubes for increasing the flow resistance. The pressures at the inlet and outlet of the parallel tubes were measured, and their results indicated that the distribution of the pressure difference for the tubes is more uniform with respect to higher flow resistances.

Kubo and Ueda [8] also inserted various sizes of orifice (2, 4, 6, and 8 mm) into the parallel tubes for changing the flow resistance. The higher resistance with smaller orifice in the parallel tubes gives better flow distribution.

1.2.5. Gravity effect

The gravity had been reported to cast a significant effect on the two-phase distribution in horizontal manifolds with vertical parallel tubes [9] due to uneven gas-liquid distribution in tubes with very high density difference between both phases. The effect of gravity to single-phase flow distribution could be much less than two-phase flow due to the parallel tubes all filled with liquid. However, it is well known that the vertical up flow decreases the local pressure along the flow path, while the vertical down flow increases the local pressure. The gravity still has a minor effect on single-phase distribution in horizontal, vertical up and vertical down flows in the parallel tubes at various flow conditions.

2. Objective of the study

The literature survey reveals that the flow distribution in a configuration of header – parallel channels is very complex. Distribution of the flow into each parallel channel is not only a function of the flow conditions in the header, but is also affected by the geometric size of the header and the parallel tubes, as well as the flow direction. In addition, the flow distribution problem may become even more critical in modern compact/micro heat exchangers. Severe flow mal-distribution could lead to overheating and cause entire failure of the thermal system. In this regard, the purpose of this study is to investigate the flow distribution subject to small and parallel tubes applicable for compact/micro heat exchangers. Investigations include the influences of Z-type and

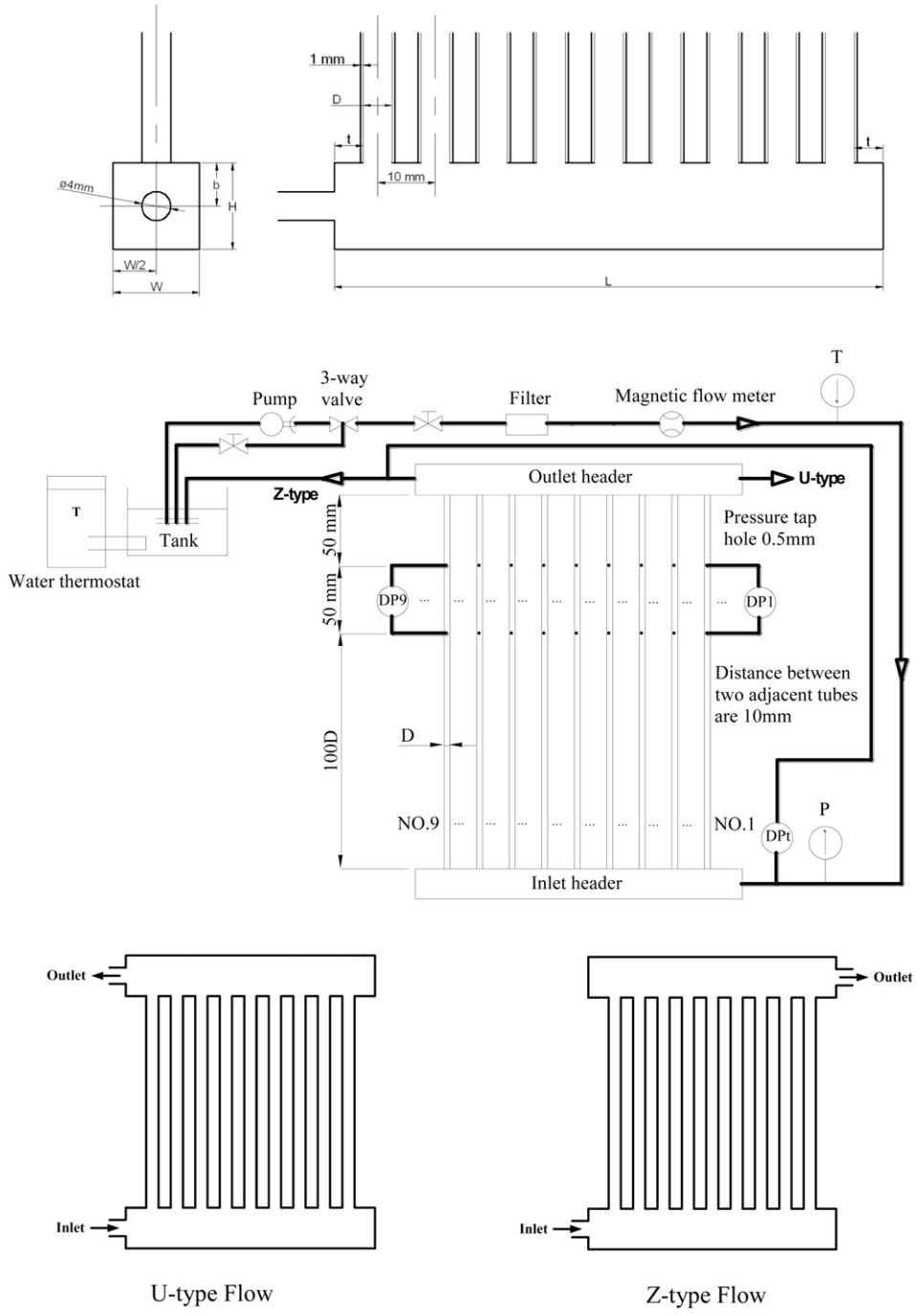

Fig. 1. Schematic diagram of the test apparatus.

U-type flow directions at horizontal, vertical up and vertical down orientations with typical headers. The effects of inlet flow conditions, channel and header sizes are also investigated with various area ratios for optimizing the flow distribution. For comparison and better into physical insight of the flow distribution, a commercial software is also utilized to simulate the pressure and flow fields.

3. Experimental apparatus

3.1. Test rig

The test rig is primarily consisted of the water circulation and test section, as well as the measurement devices depicted in Fig. 1. Water is heated by a thermostat where water is maintained at 25 °C. The water flow loop includes a variable speed gear pump. Part of the water flow is circulated through the three way valve for flow rate control. The filter is designated to remove the impurities from the stream. A very accurate Yokogawa magnetic flow meter (AXF005G) is installed at the downstream of the gear pump for measuring the water flow rate. The accuracy of water flow meter is within ±0.045 L/min of the test span. Leaving the flow meter, the water temperature is measured by a resistance temperature device (Pt100 Ω) having a calibrated accuracy of 0.1 K. The water temperature is near 25 °C during the tests. The pressure entering the test section is measured by a YOKOGAWA EJX pressure transducer with an accuracy of 0.025%. Also, a YOKOGAWA EJ110

differential pressure transducer having an adjustable span of 1300–13 000 Pa installed across the inlet of the upstream header and outlet of the downstream header with a resolution of 0.3% of the measurements.

The test section includes an inlet and outlet headers along with 9 parallel tubes as shown in Fig. 1. The foremost tube to the inlet location of header is termed 1st tube, and the aftermost one is termed 9th tube. The pressure drop for each tube at the location with 50 mm from the outlet header is measured by a YOKOGAWA EJ110 differential pressure transducer. Also, a 100 diameter calming tube length from the inlet header is used to ensure fully developed flow. The pressure taps are vertically drilled with a diameter of 0.5 mm. Leaving the test section, the water flows back to the thermal tank for recirculation.

The measurement of pressure drop in each tube is used to calculate the flow rates among the tubes. The total pressure drop includes gravitational drop ($\Delta P_g = \rho g h$) and frictional drop ΔP_f, i.e.,

$$\Delta P_T = \Delta P_f + \Delta P_g \tag{3}$$

$$\Delta P_f = 4f\frac{\Delta L}{D}\frac{G^2}{2\rho} \tag{4}$$

Where D: inner tube diameter, ΔL: tube length for ΔP measurement (50 mm), f: Fanning friction factor, ρ: density and G: mass flux. With the measured ΔP for each tube, the mass flux (G_i) and volume flow rate ($Q_i = G_i A/\rho$) could be calculated. The uncertainty of the calculated volume flow rate (Q_i) from the pressure drop is estimated to be 1.34%. The derived uncertainty of the flow ratio β and non-uniformity Φ is 2% and 3.88%, respectively. Detailed calculation of the uncertainty is shown in the Appendix.

3.2. Test sections

The test section consists of a distribution inlet header, 9 parallel tubes and an outlet header as shown in Fig. 1. The tubes and headers are made by transparent glass and acrylic fabric, respectively, for flow visualization. The geometric sizes of the test sections with a simplified schematic diagram are given in Table 1. The lengths of the parallel tubes are 300 mm and 400 mm, respectively, for 2 and 3 mm inner diameters with a pitch of 10 mm. The tube thickness for the 2 and 3 mm tubes is 1 mm. Three header sizes with square cross section of 7 mm × 7 mm, 9 mm × 9 mm and 12 mm × 12 mm were tested. The inlet flow tube to the header has an inner diameter of 4 mm. The inlet tube is located near the center position of the cross section area of the inlet header, but the vertical distance between the center position of the inlet tube to the header entrance and the parallel tubes has a vertical distance, "b", which is equal or greater than $H/2$ as shown in Fig. 1, where H is the height of the header. Since $b \geq H/2$, it indicates that the inlet tube is located at the center of the header or below it from 0 to 1.5 mm. To study the effect of velocity distribution in the header on the flow distribution, several blocks with a length of 5 mm with identical cross section area of header were used to change the distance, "t", between the inlet surface of the header entrance and the first tube, as well as the bottom surface to the last tube in the inlet header Fig. 1. The original length (L) of the flow path in the headers is 120 mm. The blocks have a hole exactly match the 4 mm hole at the entrance to the header from the inlet tube. Three different values of distance (t) are 18.5, 13.5 and 3.5 mm for the test sections with the header size of 9 mm × 9 mm and the tube size of 3 mm as shown in Table 1. Also, there are 6 values of area ratio (AR) for the combination of different sizes of tube and header for testing.

Table 1
The geometric sizes of the test sections.

D mm	H (mm)	W (mm)	AR	t (mm)	b (mm)	L (mm)
3	12	12	0.442	18.5	6	120
	9	9	0.785	18.5	5	120
				13.5		110
				3.5		90
	7	7	1.298	18.5	5	120
2	12	12	0.196	19	6	120
	9	9	0.349	19	5	120
	7	7	0.557	19	5	120

4. Results and discussion

The flow ratios (β) of the 9 parallel tubes for the vertical up flow are given in Fig. 2(a)–(f) with header sizes being 7 × 7, 9 × 9 and 12 × 12 mm for Z-type and U-type flow arrangements with the original header length (L = 120 mm). Each figure also shows flow ratio for the volumetric flow rates of 0.5, 1 and 2 L/min having 2 and 3 mm inner diameter for the parallel tubes. Apparently, the flow distribution for U-type flow is comparatively uniform than Z-type due to a more uniform pressure difference distribution across the parallel tubes between the inlet and outlet headers. In the meantime, the Z-type flow has less flow ratio in the first parallel tubes near the header entrance and a higher flow ratio distributed to the last tubes of header. The ratio between the least and the highest flow ratios for Z-type arrangement can be as high as 200% as shown in Fig. 2(d). It should be mentioned that these two configurations (Z & U) had a very dramatic difference in flow distribution. The flow ratio is increased monotonically from the first tube to the last tube while a plateau of flow distribution is seen somewhere in-between the first and last tube. The results are in line with the theoretical calculations by Bassiouny and Martin [10,11] who investigated the flow distribution and pressure drop for U-type and Z-type plate heat exchangers. For Z-type plate heat exchanger, their calculation indicated that the pressure drop amid the intake conduit and exhaust conduit is always increasing from the first tube, suggesting the rise of velocity from the first to the last tube. For the U-type configuration, the pressure difference may be approximately fixed, monotonically increased or monotonically decreased depending on characteristics parameter of the plate heat exchanger.

Notice that the 2 mm tube has a better flow distribution than that of 3 mm tube due to higher flow resistance. The results had been confirmed from some measurements and theoretical calculations (e.g. Osakabe et al. [1], Lu and Wang [12]). On the other hand, the flow distribution for 0.5 L/min is more uniform than those of 1 and 2 L/min, respectively. One of the possible explanations for this phenomenon is attributed to the entry flow pattern into the header. When the flow enters a sudden enlargement cross section at the intake conduit, single jet flow may form when the velocity is sufficient high. The momentum of the jet flow lowers its static pressure at the upper stream, thereby reducing the effective pressure difference amid the inlet and outlet headers. As a consequence, the flow ratio is decreased for the branching tubes nearby the entry.

The non-uniformities (Φ) for Z-type and U-type flow directions verse the variation of flow rate are respectively given in Fig. 3. The effects of header size and tube diameter are also included in Fig. 3, but the header length is fixed at L = 120 mm. As shown in the figure, Φ increases monotonically with the rise of flow rate for 3 mm branching tube. By contrast, Φ is marginally increased as flow rate increased from 0.5 to 1 L/min, followed by a slight decrease with a further increase of volumetric flow rate to 2 L/min. Roughly speaking, Φ is relatively insensitive to the change of volumetric flow rate when the tube diameter is reduced to 2 mm. The major

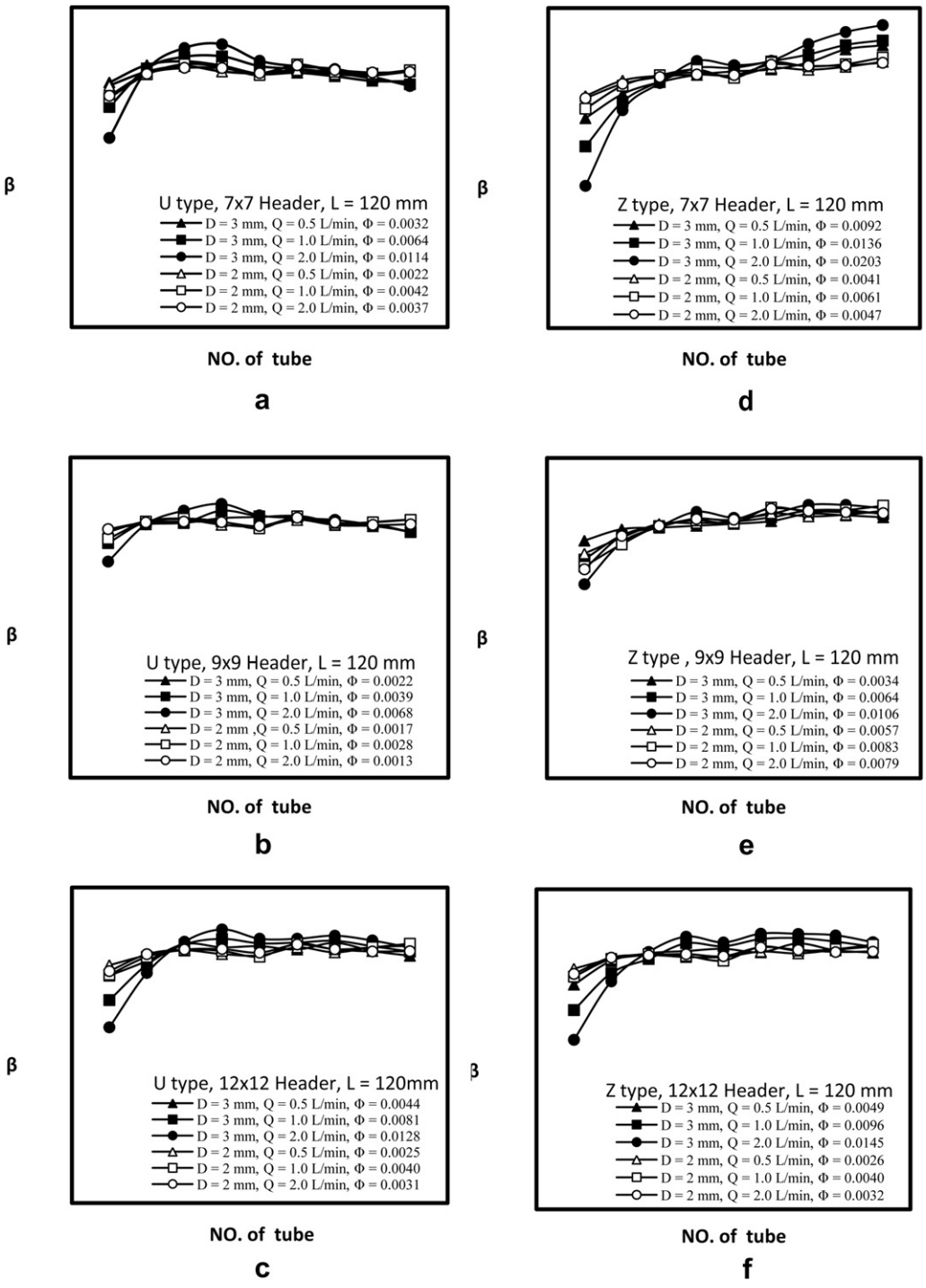

Fig. 2. Flow ratio verse No. of tube for U-type and Z-type arrangements.

explanation for this phenomenon is associated with the increase of viscous friction for smaller diameter tube as explained in preceding discussion. Additional reason is that the flow pattern in the parallel tubes had been changed from laminar flow to turbulent flow as total flow rate reached 2 L/mm since the value of friction factor is momentously increased at the flow transition. The flow resistance in these tubes at turbulent flow (higher flow rate) is higher than the tubes at laminar flow (smaller flow rate). Thus, more fluid would distribute to the tubes with smaller resistance, and thus the flow distribution is improved with a smaller Φ. The increase of flow resistance in parallel tubes would improve the flow distribution. For the same flow rate, the flow resistance of 2 mm tube is about 5 times of 3 mm tube, thus, the value of Φ for 2 mm tube at 2 L/min is much less than that of 3 mm as shown in Fig. 3 which indicates the better flow distribution for 2 mm tubes, and the results also suggest that laminar flow may have a more severe mal-distribution problem. For both U-type and Z-type configurations, the effect of the tube size on the flow distribution is analogous but is different in magnitude as shown Fig. 3. The better flow distribution in U-type flow with smaller non-uniformity (Φ) is due to the uniform

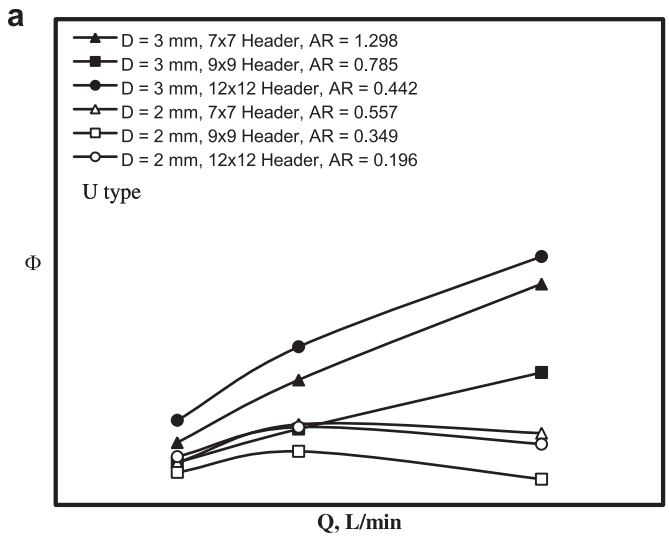

Fig. 3. Non-uniformity Φ vs. volumetric flow rate subject to Z-type and U-type arrangements.

pressure change distribution between the inlet and outlet of the parallel tubes.

For verifying the entrance effect in the header, the length of flowing path for the header was modified by inserting blocks with a dimension of 5 × 9 × 9 mm into the 9 × 9 mm header. Thus, the distance (t) between the inlet location and the first tube had been reduced from 18.5 mm to 13.5 mm and 3.5 mm, respectively while the header length (L) was changed from 120 mm to 110 mm and 90 mm, respectively. The lengths of L and t are also given in Table 1. The results of flow ratio of the 9 parallel tubes subject to the effect of entrance length (t) for Z-type flow in 3 mm tubes are given in Fig. 4(a). By increasing the entrance length (t), the flow distribution is generally improved. The shorter entrance is prone to mal-distribution, yet this phenomenon becomes more severe when the inlet volumetric flow rate is increased. Normally the flow rate (or flow ratio) is the lowest in the first tube, and is gradually increased as the tube number increased. The results are explained in the foregoing discussion where the jet flow phenomenon is more conspicuous with the inlet volumetric flow rate. The non-uniformity (Φ) verse the effect of entrance length (t) for Z-type flow is also shown in Fig. 4(b). For the same volumetric flow rate, the values of Φ for $L = 90$ mm are much higher than those of $L = 110$ and 120 mm, indicating a much severe mal-distribution problem associated with $L = 90$ mm. With a shorter entrance length, the developed jet flow may considerably influence the flow distribution of the first several tubes. Conversely, with the rise of entrance length, the effect of jet flow is eased appreciably. The relation of non-uniformity (Φ) against the inlet volumetric flow is proportional to $Q^{0.669}$.

The effect of gravity on the flow distribution had been studied for Z-type flow with the present 9 × 9 mm header and 3 mm parallel tubes. Tests are conducted for vertical up, vertical down and horizontal arrangements and results are depicted in Fig. 5. As seen in the figure, the flow ratio is quite insensitive to change of orientation. For an easier comparison, the values of non-uniformity (Φ) for various orientations at different volume flow rates are plotted in Fig. 6. The values of non-uniformity (Φ) for the vertical down orientation are marginally higher than the other two

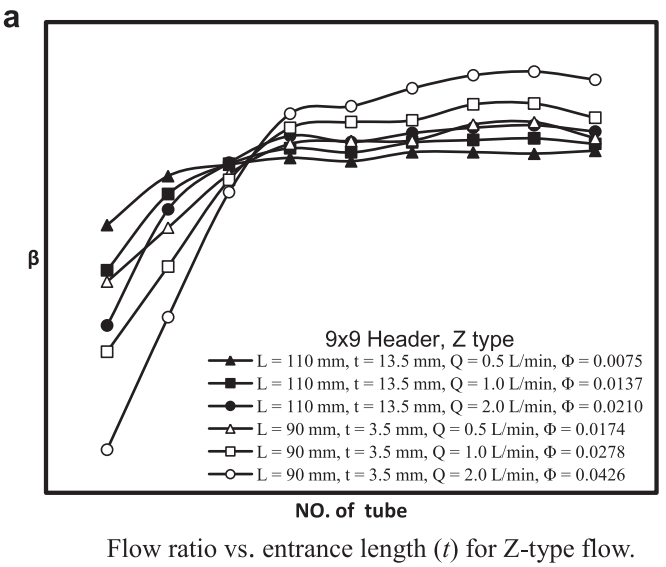

Fig. 4. Effect of entrance length on the flow distribution of Z-type arrangement.

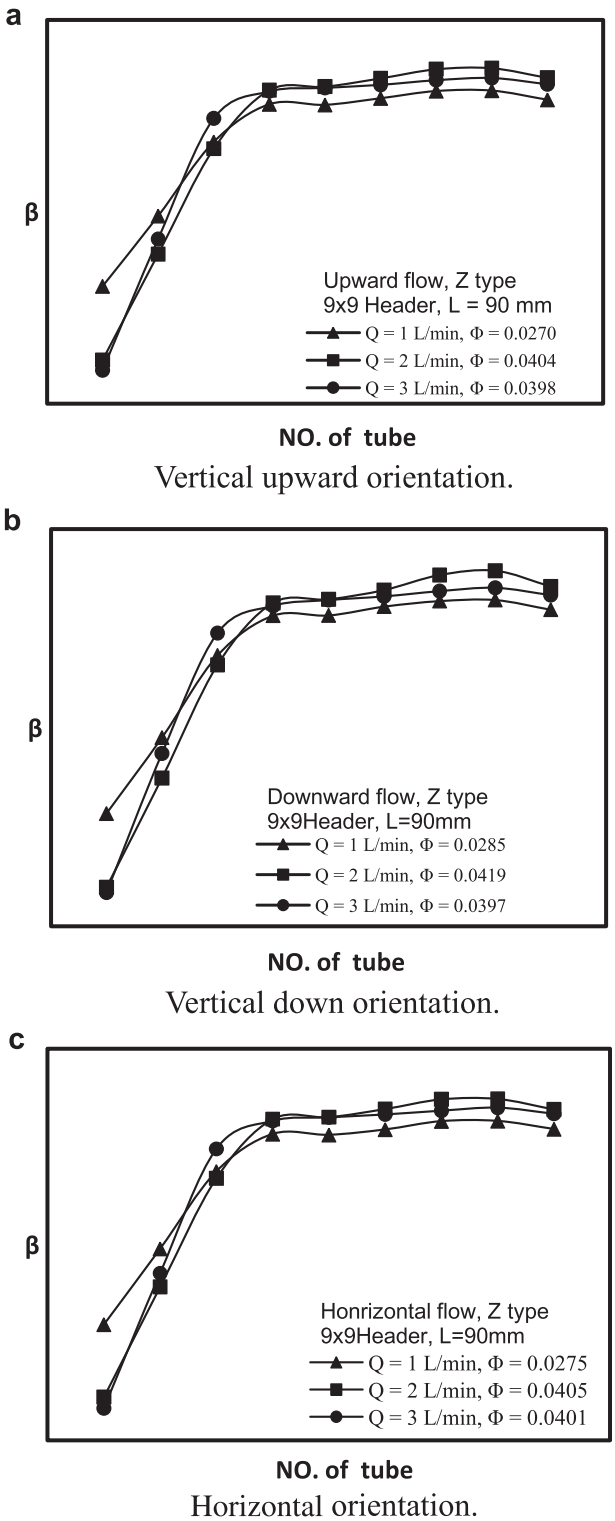

Fig. 5. Flow distribution with Z-type flow for various orientations.

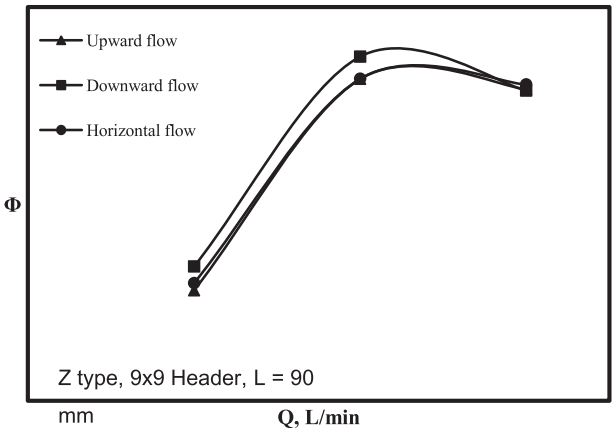

Fig. 6. Non-uniformity (Φ) for various orientations.

orientations for $Q = 1$ and 2 L/min. At $Q = 3$ L/min, non-uniformity is nearly the same amid the three orientations. Most of the tubes are in the laminar flow regime for $Q = 1$ and 2 L/min where gravity still could impose a very small effect on flow distribution, especially, for the vertical down orientation. For $Q = 3$ L/min, the flow regime moves toward transition/turbulent flow where the friction resistance takes control, thereby the influence of gravity becomes insignificant.

For a better understanding of the flow distribution characteristics in compact parallel flow heat exchangers at different flow conditions, test results are compared with simulation from the EFD.lab commercial software. The simulation is based on the 9×9 mm headers having $L = 90$ mm with vertical up flow in U-type and Z-type flow directions. The parallel tubes have a diameter of 3 mm. Fig. 7 shows the simulation vs. the experimental results for $Q = 1$ and 2 L/min in Z-type flow direction. The calculated results are in good agreement with the experimental results, and the calculated values of non-uniformity (Φ) from the simulation and the experiment are 0.0239 and 0.0245, respectively, for $Q = 1$ L/min Figs. 8, 9 and 10 depict the velocity and pressure contours, as well as the flow velocity lines, respectively, with $Q = 2$ L/min in 90 mm header and 3 mm parallel tubes in U-type flow direction. As shown in Fig. 8, a clear jet flow pattern presents at the entrance, yet the higher velocity at the header inlet is then gradually decreased along the conduit. Also, the first several tubes have the smallest lateral flow velocity, while the last one has the

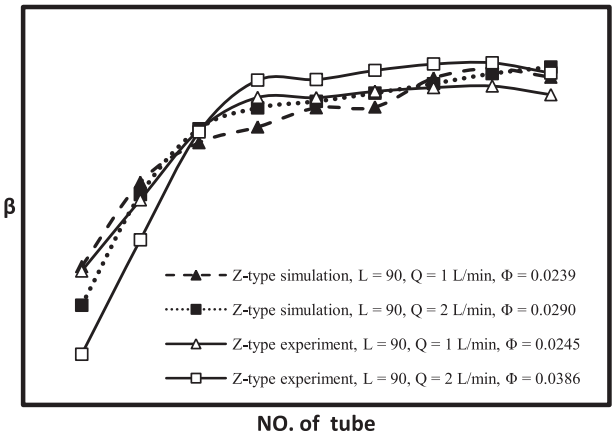

Fig. 7. Numerical simulation of flow ratio for Z-type flow vs. data.

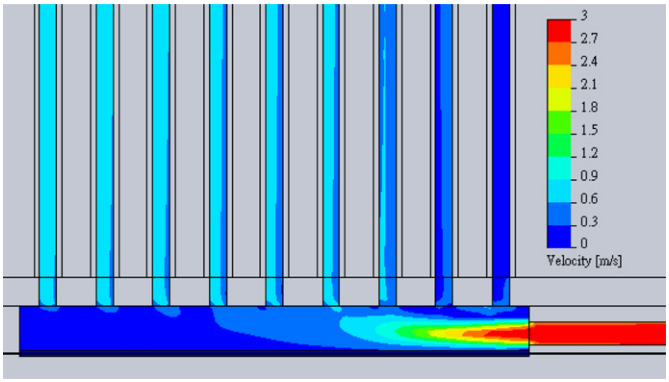

Fig. 8. Velocity simulation in 9 × 9 mm header with 90 mm length and $D = 3$ mm tubes.

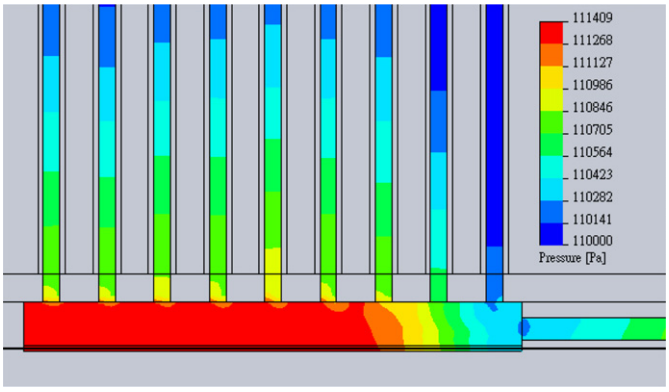

Fig. 9. Pressure simulation in 9 × 9 mm header with 90 mm length and $D = 3$ mm tubes.

highest flow velocity. Due to the jet effect at the entrance, the pressure is smallest at the entrance and is largest at the end of the header as shown in Fig. 9. Thus, the first tube near the entrance has the lowest pressure and the tube pressure is increased with the increase of tube number. Fig. 10 shows the flow velocity lines in the front four and the header inlet. The result shows the jet flow is induced at the header inlet with a clear vortex circulated at the sides of the expanded jet flow. Also, a small eddy flow is observed near the inlet of the first tube due to the circulation of the vortex flow. This vortex flow would reduce the flow rate of the first tube. Similar calculations were also reported by Fu et al. [13] who showed a secondary flow is generated at the inlet of the first tube.

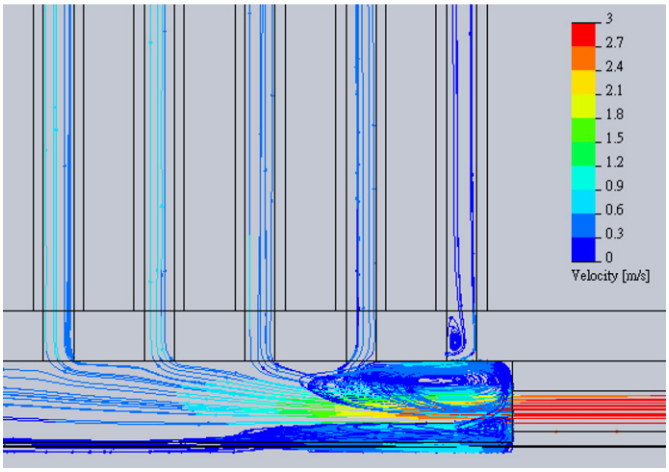

Fig. 10. Simulation of flow velocity lines in the header entrance and the front tubes.

5. Conclusion

The single-phase flow distribution in compact parallel flow heat exchanger is investigated by experiments and numerical simulations subject to various operating conditions. The flow rates for all 9 parallel tubes are calculated by the measured pressure drops, the results are summarized as the following:

1. As total flow rate increases, the jet flow phenomenon becomes more pronounced, yielding smaller pressure difference for the first several branching tubes between the intake and exhaust conduit. Therefore, a substantial reduction of flow rate in the first several tubes is observed. The mal-distribution caused by jet flow at the sudden expansion of the header is considerably eased by exploitation of a smaller diameter branching tube. Alternatively, the mal-distribution at the first several tubes can be significantly improved by using a settling entrance length.
2. The gravity casts a very small effect on the flow distribution. The non-uniformity is slightly higher for vertical down flow with smaller flow rate. As the flow rate increases, the tube flow resistance also increases, thus, the gravity effect becomes insignificant.
3. The flow distribution for U-type flow is more uniform than Z-type flow.
4. The trends of the local flow ratios between the simulations and experiments are very similar but with a small deviation of non-uniformity.
5. The numerical results clearly indicate a jet flow is generated with circulated vortex flow at the header inlet, as well as a small eddy flow at the inlet of the first tube that would reduce the flow rate to the first tube.

Acknowledgements

The grant from National Science Committee (NSC 98-2221-E-224-049) of Taiwan is appreciated for supporting this study. Also, the authors are indebted to financial support from the Bureau of Energy of the Ministry of Economic Affairs, Taiwan.

Appendix. Detailed calculation of the uncertainty

From the pressure drop formula and relation between volumetric flow rate and mass flux,

$$\Delta P = 4f\frac{L}{D}\frac{G^2}{2\rho} \tag{A1}$$

$$G = \frac{Q\rho}{A} \tag{A2}$$

Hence

$$Q = \left(\frac{\Delta P D A^2}{2fL\rho}\right)^{\frac{1}{2}} \tag{A3}$$

Therefore the uncertainty of Q is obtained from the following

$$\delta Q = \left[\left(\frac{\partial Q}{\partial \Delta P}\delta\Delta P\right)^2+\left(\frac{\partial Q}{\partial D}\delta D\right)^2+\left(\frac{\partial Q}{\partial A}\delta A\right)^2+\left(\frac{\partial Q}{\partial L}\delta L\right)^2\right]^{\frac{1}{2}}$$

$$= \left[\left(\frac{1}{2}\left(\frac{\Delta PDA^2}{2fL\rho}\right)^{\frac{-1}{2}}\times\frac{DA^2}{2fL\rho}\times\delta P\right)^2 + \left(\frac{1}{2}\left(\frac{\Delta PDA^2}{2fL\rho}\right)^{\frac{-1}{2}}\times\frac{\Delta PA^2}{2fL\rho}\times\delta D\right)^2 + \left(\frac{1}{2}\left(\frac{\Delta PDA^2}{2fL\rho}\right)^{\frac{-1}{2}}\times\frac{2D\Delta PA}{2fL\rho}\times\delta A\right)^2 + \left(\frac{1}{2}\left(\frac{\Delta PDA^2}{2fL\rho}\right)^{\frac{-1}{2}}\times\frac{\Delta PDA^2}{2fL^2\rho}\times(-1)\times\delta D\right)^2\right]^{\frac{1}{2}} \quad (A4)$$

Employing the measured accuracies of the primary measurements (pressure drop, Employing the measured accuracies of the primary measurements (pressure drop, diameter, tube length, area.) to the derived parameter Q, one can estimate the associate uncertainty as $\delta Q \approx 0.000653$

$$U_Q = \frac{\delta Q}{Q} \approx 0.0133 \approx 1.33\%$$

As a result, estimation of β_i is conducted with similar procedures:

$$\beta_i = \frac{Q_i}{Q_{\text{total}}} \quad (A5)$$

$$\delta\beta_i = \left[\left(\frac{\partial\beta}{\partial Q_i}\delta Q_i\right)^2+\left(\frac{\partial\beta_i}{\partial Q_{\text{total}}}\delta Q_{\text{total}}\right)^2\right]^{\frac{1}{2}} = \left[\left(\frac{\delta Q_i}{Q_{\text{total}}}\right)^2+\left(\frac{-Q_i}{Q_{\text{total}}^2}\delta Q_{\text{total}}\right)^2\right]^{\frac{1}{2}} \quad (A6)$$

Therefore,

$$\delta\beta_i \approx 9.9\times10^{-4}$$

$$U_{\beta_i} = \frac{\delta\beta_i}{\beta_i} \approx 0.02 \approx 2\%$$

Similarly, the uncertainty of Φ is given in the following:

$$\Phi = \frac{\sqrt{\sum_i^N(\beta_i-\overline{\beta})^2}}{N} \quad (A7)$$

$$\overline{\beta} = \frac{\sum_i^N\beta_i}{N} = \frac{\beta_1+\ldots\beta_9}{9} \quad (A8)$$

$$\delta\overline{\beta} = \left[\left(\frac{\partial\overline{\beta}}{\partial\beta_1}\delta\beta_i\right)^2+\ldots\left(\frac{\partial\overline{\beta}}{\partial\beta_9}\delta\beta_i\right)^2\right]^{\frac{1}{2}} \quad (A9)$$

$$\delta\overline{\beta} \approx 3.3\times10^{-4}$$

$$\delta\Phi = \left[\left(\frac{\partial\Phi}{\partial\beta_i}\delta\beta_i\right)^2+\left(\frac{\partial\Phi}{\partial\overline{\beta}}\delta\overline{\beta}\right)^2\right]^{\frac{1}{2}} = \left[\left(\frac{1}{2}\left(\frac{(\delta\beta_i-\overline{\beta})}{N}\right)^{\frac{-1}{2}}\times\frac{2(\delta\beta_i-\overline{\beta})}{N}\times\delta\beta_i\right)^2 + \left(\frac{1}{2}\left(\frac{(\delta\beta_i-\overline{\beta})}{N}\right)^{\frac{-1}{2}}\times\frac{2(\delta\overline{\beta}-\beta_i)}{N}\times\delta\overline{\beta}\right)^2\right]^{\frac{1}{2}} \quad (A10)$$

Thus,

$$\delta\Phi \approx 0.00104$$

$$U_\Phi = \frac{\delta\Phi}{\Phi} \approx 0.0388 \approx 3.88\%$$

References

[1] M. Osakabe, T. Hamada, S. Horiki, Water flow distribution in horizontal header contaminated with bubbles, International Journal of Multiphase Flow 25 (1999) 827–840.
[2] J.P. Chiou, The effect of nonuniform fluid flow distribution on the thermal performance of solar collector, Solar Energy 29 (1982) 487–502.
[3] A.B. Datta, A.K. Majumdar, Flow distribution in parallel and reverse flow manifolds, International Journal of Heat and Fluid Flow 2 (4) (1980) 253–262.
[4] R.A. Bajura, E.H. Jones Jr., Flow distribution manifolds, Journal of Fluids Engineering 98 (1976) 654–666.
[5] S.H. Choi, Y.I. Cho, Yong, The effect of area ratio on the flow distribution in liquid cooling module manifolds for electronic packaging, International Communications in Heat and Mass Transfer 20 (1993) 221–234.
[6] J.C.K. Tong, E.M. Sparrow, J.P. Abraham, Geometric strategies for attainment of identical outflows through all of the exit ports of a distribution manifold in a manifold system, Applied Thermal Engineering 29 (2009) 3552–3560.
[7] C.C. Wang, Heat Transfer Design, in Chinese. Wunan, Taipei, 2007.
[8] T. Kubo, T. Ueda, On the characteristics of divided flow and confluent flow headers, Bulletin of JSME 12 (1969) 802–809.
[9] S. Vist, Two-phase Flow Distribution in Heat Exchanger Manifolds, Ph.D thesis, Norwegian University of Science and Technology, Trondheim, Norway, 2004.
[10] M.K. Bassiouny, H. Martin, Flow distribution and pressure drop in plate heat exchangers I; U-type arrangement, Chemical Engineering Science 39 (1984) 693–700.
[11] M.K. Bassiouny, H. Martin, Flow distribution and pressure drop in plate heat exchangers I; Z-type arrangement, Chemical Engineering Science 39 (1984) 701–704.
[12] M.C. Lu, C.C. Wang, Effect of the inlet location on the performance of parallel-channel cold-plate, IEEE Transactions on Components & Packaging Technologies 29 (2006) 30–38.
[13] H. Fu, A.P. Watkins, M. Yianeskis, The effects of flow split ratio and flow rate in manifolds, International Journal for Numerical Methods in Fluids 18 (1994) 871–886.